

Portland State University

PDXScholar

Chemistry Faculty Publications and
Presentations

Chemistry

1-2014

The Confluence of Structure and Dynamics in Lanthanide(III) Chelates: How Dynamics Help Define Structure in Solution

Benjamin Charles Webber

Portland State University, benjamin_webber@hotmail.com

Mark Woods

Portland State University, mark.woods@pdx.edu

Follow this and additional works at: https://pdxscholar.library.pdx.edu/chem_fac

 Part of the [Chemistry Commons](#)

Let us know how access to this document benefits you.

Citation Details

Published as: Webber, B.C. and Woods, M. (2014). The confluence of structure and dynamics in lanthanide(III) chelates: how dynamics help define structure in solution. *Dalton Trans.*, 43, 251–258.

This Post-Print is brought to you for free and open access. It has been accepted for inclusion in Chemistry Faculty Publications and Presentations by an authorized administrator of PDXScholar. For more information, please contact pdxscholar@pdx.edu.

Published in final edited form as:

Dalton Trans. 2014 January 7; 43(1): 251–258. doi:10.1039/c3dt52143e.

The confluence of structure and dynamics in lanthanide(III) chelates: how dynamics help define structure in solution

Benjamin C. Webber^a and Mark Woods^{*,a,b}

^aDepartment of Chemistry, Portland State University, 1719 SW 10th Ave, Portland OR 97201, USA.. Tel: +1 503 725 8238

^bAdvanced Imaging Research Center, Oregon Health & Science University, 3181 SW Sam Jackson Park Road, Portland OR, 97239, USA. Fax: +1 503 418 1543; Tel: +1 503 418 5530

Abstract

Coordination exchange processes tend to dominate the solution state behaviour of lanthanide chelates and generally prohibit the study of small conformational changes. In this article we take advantage of coordinatively rigid Eu³⁺ chelates to examine the small conformational changes that occur in these chelates as water dissociatively exchanges in and out of the inner coordination sphere. The results show that the time-averaged conformation of the chelate alters as the water exchange rate increases. This conformational change reflects a change in the hydration state (q/r_{LnH}^6) of the chelate. The hydration state has recently come to be expressed as two separate parameters q and r_{LnH} . However, these two parameters simultaneously describe the same structural considerations which in solution, are indistinguishable and intrinsically related to, and dependent upon, the dissociative water exchange rate. This realization leads to the broader understanding that a solution state structure can only be appreciated with reference to the dynamics of the system.

Introduction

The traditional picture of the dissociative solvent exchange mechanism in inorganic chemistry that was developed over four decades ago¹ may tend to limit our appreciation of such processes. It describes a situation in which the metal-solvent bond breaks forming a complex intermediate in which the coordination number is reduced by one. The solvent molecule is then replaced by another. The picture afforded by this model is completely binary: no account is taken for how the solvent molecule moves or what happens to the remainder of the metal complex during this exchange process. It is almost as if the system oscillates between two quantum states. This traditional picture of dissociative exchange in these chelates has come to dominate discourse: it is a picture in which the solution state structure is essentially static (Figure 1). Many applications demand a more rigorous

© The Royal Society of Chemistry [year]

mark.woods@pdx.edu, woodsmar@ohsu.edu.

[†]Electronic Supplementary Information (ESI) available: A description of proton assignments; an analysis of the NMR shifts of hydrated and dehydrated YbDOTA-type chelates; variable temperature ¹H NMR data for the other isomeric chelates of EuNB-DOTMA; and a stacked plot of VT ¹H NMR spectra of EuDOTP. See DOI: 10.1039/b000000x/

understanding of solution state structure and associated parameters that incorporate a dynamic component of the exchange process. One such application is use of Gd^{3+} chelates as MRI contrast agents. Dissociative exchange of water between the chelate and the bulk in the monohydrated Gd^{3+} chelates used as MRI contrast agents is known to occur through a dissociative mechanism.²

The longitudinal relaxivity (r_1) of a paramagnetic species describes its ability to shorten the T_1 of bulk water; the higher the relaxivity the more effective the agent. The inner-sphere relaxivity of an agent, arising from exchange of the coordinated water molecule, scales directly with the number of water molecules in the inner coordination sphere (q) and the negative sixth power of the distance between Gd^{3+} and the water protons ($1/r_{\text{GdH}}^6$).³ For reasons of patient safety only a single water molecule may be permitted to access the inner coordination sphere – although some potential exceptions to this limit may exist.⁴⁻⁶ In contrast to the value of q , the parameter r_{GdH} is almost completely ignored in contrast agent development and is most commonly treated as invariant. Only occasionally has this parameter been deemed worthy of consideration.⁷⁻⁹ From the theory of nuclear magnetic relaxation developed by Solomon, Bloembergen and Morgan (SBM)¹⁰⁻¹⁴ a raft of other parameters are found to influence relaxivity. Not least amongst these is the rate at which the coordinated water molecule exchanges with the bulk, often expressed in terms of the water residence lifetime ($\tau_{\text{M}} = 1/k_{\text{ex}}$). In practice τ_{M} has only a minimal effect on relaxivity until the limiting effect of τ_{R} , the rotational correlation time, is lifted. Clinical contrast agents are low molecular weight Gd^{3+} chelates and as such tumble too rapidly in solution to afford high relaxivities. Furthermore clinical agents have dissociative water exchange kinetics that are, according to SBM theory, too slow to afford the highest relaxivities. The path to highly effective contrast agents is therefore to couple accelerated dissociative water exchange with a reduction in the rate of molecular tumbling.

A number of groups have developed strategies for accelerating dissociative water exchange in monohydrated Gd^{3+} chelates.¹⁵⁻²¹ However, when these rapidly exchanging chelates are coupled with slow molecular tumbling, usually through marrying the motion of the chelate to that of a macromolecule, the gains in relaxivity are disappointing.²²⁻²⁴ Our own efforts to couple the molecular tumbling of rapidly exchanging Gd^{3+} chelates to macromolecular structures have also been disappointing,²⁵ but in our case unique insights can be gained into why the highest relaxivities are not attained. The clinical contrast agent GdDOTA exists as a mixture of two coordination isomers: the square antiprism (SAP) and the twisted square antiprism (TSAP).^{26, 27} It has long been appreciated that the TSAP isomer has water exchange kinetics that are an order of magnitude, or more, faster than the SAP isomer.^{28, 29} By appropriately substituting the DOTA ligand framework we have been able to prepare chelates of *S*-SSSS-NB-DOTMA that adopt the TSAP coordination geometry exclusively: affording chelates with very fast dissociative water exchange kinetics ($\tau_{\text{M}} = 15$ ns).³⁰ Where our approach differs from those of other groups is that, using the same methods, we are also able to prepare chelates of *S*-RRRR-NB-DOTMA that adopt the SAP coordination geometry exclusively; affording a chelate with slower (though still rapid) water exchange kinetics ($\tau_{\text{M}} = 120$ ns). This allows the effect of accelerating water exchange in slowly tumbling chelates to be compared directly.²⁵ When the molecular tumbling of these geometrically constrained

Gd³⁺ chelates is slowed the gains in relaxivity confound expectation: a slowly tumbling TSAP isomer (very fast water exchange) was found to have *lower* relaxivity than a slowly tumbling SAP isomer (moderately rapidly water exchange).²⁵ Probing these relaxivity data reveals that this result arises as a consequence of a parameter that scales directly with relaxivity at all magnetic fields³: either q or $1/r_{\text{GdH}}$.⁶

The value of r_{GdH} is difficult to access directly particularly in solution. Caravan and co-workers have proposed that ENDOR can be used to probe this value directly,⁹ but this technique requires that the chelate be frozen in a glass and cannot therefore provide a value representative of the solution state at room temperature. Crystallography allows direct access to the value of r_{GdO} , but because the positions of the water hydrogen atoms are poorly defined it does not permit an accurate value of r_{GdH} to be obtained. Moreover, the major limitation of these approaches is that they are solid state techniques that consider the *structure* of the chelate in the solid state but they take no account of the dynamics inherent to the system when in solution. The values of r_{GdH} (or r_{GdO}) determined by these techniques may not accurately reflect the value in solution. Nonetheless, the crystal structures of GdDOTMA and GdTCE-DOTA provide some insight into differences in the metal-water distance in the two coordination isomers of DOTA-type chelates. GdTCE-DOTA crystallizes in the SAP coordination geometry and has $r_{\text{GdO}} = 2.431 \text{ \AA}$.²⁸ In comparison GdDOTMA crystallizes in the TSAP coordination geometry and has $r_{\text{GdO}} = 2.50 \text{ \AA}$,³¹ an elongation of the metal water bond of 2.8% over the SAP isomer. Presumably this difference in r_{GdO} affects the lability of the Gd-O bond and is the origin of the faster water exchange kinetics in the TSAP isomer.

It is widely accepted that Eu³⁺ can be used as a surrogate for Gd³⁺ to probe chelate structure because both elements lie adjacent in the lanthanide series and are of similar size, but Eu³⁺ has electronic properties that are generally more amenable to structure elucidation methods. We have previously reported the hydration states of isolated coordination isomers of EuNB-DOTMA in solution,³² using a revised Horrocks' method.³³ This approach afforded a somewhat different picture of the metal water distances in the two chelates.³² The hydration state, q^{SAP} was determined to be 0.97, whereas q^{TSAP} was found to be considerably smaller: 0.74.³² This difference may be interpreted by invoking a population distribution for the TSAP isomer in solution with about ³/₄ of the sample mono-hydrated and ¹/₄ dehydrated. This population distribution idea has been invoked¹⁹ to explain some of the observed coordination chemistry of chelates some of the smaller rare earths, but **never** those of lanthanides in the middle of the series such as Eu³⁺ or Gd³⁺. The notion of a distribution of hydration populations is sometimes erroneously interpreted to mean that a dehydrated form exists either discretely or in slow exchange with the hydrated form. As shown in the supporting information this reasoning is not consistent with the observation of a single species in the ¹H NMR spectra of the Eu³⁺ chelates (this work) or Yb³⁺ chelates³⁴ (supplementary information S2). Water exchange is very fast on the NMR (and even luminescence) time-scale and so the species observed in the NMR spectrum is the weighted time-average of the hydrated and dehydrated forms.

The observed discrepancy in the hydration state of the two isomeric Eu³⁺ chelates can, however, be fully understood by considering Parker's seminal 1999 paper on lanthanide

hydration.³³ The key realization is that the quenching of Eu^{3+} excited states by proximate OH oscillators also has a $1/r_{\text{EuH}}^6$ dependence. Thus the value of q determined by Horrocks' method reflects not only the number of water molecules but also their distance from the metal ion. We previously³² used this realization and equation 1 to undertake a rather naïve calculation which points to an increase in r_{EuO} in solution of 4.5% longer in the TSAP isomer over the SAP isomer.³² This affords a value of r_{EuO} of about 2.6 Å for the TSAP isomer, much longer than observed in the crystal.

$$\frac{r_{\text{TSAP}}}{r_{\text{SAP}}} = \left(\frac{q_{\text{SAP}}}{q_{\text{TSAP}}} \right)^{-6} \quad (1)$$

The discovery that the difference between the metal-water distances of the SAP and TSAP isomers appears to be larger in solution than in the crystal is not entirely surprising. Exchange effects are absent from the crystal but must play important roles in the structure of molecules in solution. This raises the question of whether altering the dissociative water exchange dynamics can *cause* a change the hydration state of a lanthanide ion in solution. It has already been established that changes in dissociative water exchange kinetics are the *effect* of longer “metal water bonds” (*i.e.* in the crystal).³⁵ This question takes on increased importance in light of our recent discovery that the decreased hydration state observed for a TSAP Gd^{3+} chelate has a profoundly limiting effect upon relaxivity when molecular tumbling is slowed despite almost “optimal” water exchange kinetics.²⁵

Results

It is now known that a single stereoisomer of the ligand NB-DOTMA can form two possible regioisomeric chelates with Eu^{3+} or Gd^{3+} . These regioisomers, which have been described in detail elsewhere,^{36, 37} are defined as ‘corner’ and ‘side’ isomers depending upon the location of the nitrobenzylic substituent on the macrocycle. The formation of the two regioisomers occurs during introduction of the metal ion into the ligand and therefore preparation of one regioisomer of a geometrically constrained chelate necessarily affords the other and the two must be separated by preparative RP-HPLC. As part of our investigations into the chemistry of these regioisomeric chelates we undertook a series of variable temperature ^1H NMR studies on the conformationally constrained Eu^{3+} chelates.

The paramagnetic Eu^{3+} ion induces large hyperfine shifts in the ligand protons, arising from a contact and a dipolar contribution.³⁸ The sign and magnitude of the dipolar contribution is directly related to the position of the proton relative to the metal ion, according to equations 2 and 3. In Eu^{3+} some protons experience a sizable contact contribution that does not relate to the position of the proton. This precludes a complete quantitative shift analysis of the type that is often undertaken for Yb^{3+} chelates. However, it has been shown that the most shifted protons – the axial ring protons, ax^S , and the pendant arm protons, ac – in a EuDOTA-type chelate experience almost no contact contribution.^{39, 40} As a consequence the shifts of these protons can be used to provide qualitative insights into chelate conformation. From examination of the variable temperature data (Figure 2) it appears that the shifts of the ax^S and ac protons exhibit different temperature dependencies. As the temperature increase the

LIS of all proton resonances decreases as the value of D decreases. This is primarily the result of the presence of a temperature term in equation 3 but also arises because of thermal population of low lying excited states reducing the value of C_j . However, the change in shift is not uniform: those of the ac and ax^S protons change at different rates with changing temperatures for all six isomeric chelates of EuNB-DOTMA (Figure 3; data for the diastereoisomeric S -RRRR and S -SRRR-NB-DOTMA chelates, both SAP isomers,³⁷ are provided in the supplementary information, S3-S6). This suggests a temperature dependent conformational change in these chelates. The shifts of the same protons in EuDOTP, which does not possess a coordinated water molecule, change at a uniform rate consistent with the chelate maintaining the same conformation over this temperature range. It is clear that the conformational changes observed in the EuNB-DOTMA chelates are related to changes in the dissociative water exchange kinetics. It is noteworthy that the two TSAP isomers of EuNB-DOTMA, which exchange most rapidly, exhibit a greater divergence of the ax^S and ac protons shifts over this temperature range than do the four more slowly exchanging SAP isomers. The location of the nitrobenzyl group appears to have little or no effect on these changes.

Discussion

Hermann and Lukeš were the first to realize that the traditional picture of dissociative exchange in Ln^{3+} DOTA-type chelates is incomplete in one key respect: the traditional model holds the chelate structure firm through the dissociative exchange process: *i.e.* there is no conformational change. The unusual crystal structure of YDO3AP(ABn) stimulated these researchers to survey the crystallographic literature of mono- and dehydrated LnDOTA-type chelates.⁴¹ One characteristic stood out, the metal ion was always found deeper in the coordination cage, closer to the aza-crown, in dehydrated chelates than it was in monohydrated chelates. This led to the hypothesis that the metal ion was in fact moving up and down within the coordination cage as the water molecules came and went. The stimulus for this motion is presumably demand for electron density, which when not satisfied by a coordinated water molecule has to be, at least partially, satisfied by a move closer to the macrocyclic nitrogen donor atoms. Concerted movement of the metal ion within the coordination cage with water exchange is consistent with more recent crystallographic evidence obtained on partially hydrated chelates.⁴² It would also explain the results of the variable temperature NMR experiments presented above. The crystal structure of YDO3AP(ABn) affords the structures of three coordination modes in a single unit cell. Of particular interest are the two TSAP isomers of which one is monohydrated and the other completely dehydrated. These two structures represent the extremes of the dissociative exchange model and therefore describe the conformational changes that occur within the chelate during water exchange. Some of the structural parameters of these two chelates are summarized in Table 1. These data show that as the water molecules come and go the associated motion of the metal ion within the coordination cage causes the ligand to “breathe” in manner similar that found in molecular dynamic simulations of related chelates.⁴³ The ligand contracts as water leaves and opens up again as water returns.

The position of the ac protons in YDO3AP(ABn) relative to the metal ion does not vary substantially between the hydrated and dehydrated structures (Table 1). In contrast the

position of the ax^S protons change considerably, moving up and towards the metal as the chelate loses water. This change in position will be reflected in the dipolar contribution of the chemical shifts of these protons. The axial dipolar component, which by inspection of the NMR spectra can be seen to predominate, is defined by equations 2 and 3:

$$\delta_{ax}^d = D \left(\frac{3 \cos^2 \theta - 1}{r^3} \right) \quad (2)$$

$$D = B_2^0 \frac{C_J \mu_B^2}{60(kT)^2} \quad (3)$$

where D is a chelate specific ligand field parameter.³⁸ This allows the shifts of the ax^S and ac protons to be considered in terms of r and θ , a relationship more conveniently expressed by the geometric parameter, G (Table 1). From the values of G calculated from the crystal (Table 1), it is apparent that the hyperfine shift of the ac protons is relatively unaffected on passing from a hydrated to a dehydrated form of the chelate. In contrast the ax^S protons will experience a substantial increase in their hyperfine shifts. For EuDOTP there is no hydration equilibrium and therefore no conformational change with changing temperature and the shifts of both the ac and ax^S protons follow the same temperature dependence. In all EuNB-DOTMA chelates the shifts of the ac protons track the changes in shift of EuDOTP closely changing in accordance with the temperature dependence of the dipolar shift. The shifts of the ax^S protons do not decrease at nearly the same rate, indicating a conformational change that increases the value of G as water exchange gets faster. This implies that as the temperature of the sample is increased the time-averaged conformation of these chelates changes from something close to the mono-hydrated form, to something that possesses more character from the dehydrated form (Figure 4).

These results are surprisingly easy to rationalize in terms of the traditional dissociative exchange model. Because dissociative exchange is very fast on the NMR time-scale there are two ways in which these results can be viewed, either: as the result of exchange on the entire ensemble of chelates viewed in a single instant; or as the effect of exchange on a single chelate over the period of observation. The ergodic principle may be applied. A critical realization must first be made however: the lifetime of the dehydrated state of the chelate cannot be infinitely short. The lifetime of dehydrated chelate is undoubtedly very short. As a consequence when τ_M is long, the time each chelate spends in a dehydrated state is insignificantly small and we say that:

$$1/k_{ex} = \tau_M \quad (4)$$

However, when τ_M becomes very short the lifetime of the dehydrated chelate becomes significant relative to τ_M . In this situation the time taken for exchange ($1/k_{ex}$) is the sum of the lifetimes of the hydrated (τ_M) and dehydrated states. In short equation 4 no longer holds true. With that in mind we can imagine a snap-shot of an ensemble of chelates undergoing slow dissociative water exchange. The vast majority of the chelates will have a water

molecule close to the metal ion. A small fraction of the chelates will have no water molecule close to the metal ion. Now if the rate of dissociative water exchange is increased this dehydrated fraction will increase. We can see that the hydration *number* observed for the ensemble is intrinsically linked to the exchange rate. But what of those chelates that have a water molecule that lies somewhere between associated and dissociated, *i.e.* in the process of exchange? Intuitively this fraction will also grow as dissociative exchange accelerates. The chelates in this fraction can neither be characterized as hydrated nor dehydrated.⁴⁴ These chelates can only be characterized by averaging the distances of all these water molecules from the metal ion. In other words, careful consideration also reveals that the apparent *distance* of the water molecule from the metal will also be simultaneously affected by change in the rate of dissociative exchange. This concept can equally be understood on the basis of changes in hydration of a single chelate over a period of observation. Figure 5 attempts to illustrate this. It shows the changes in hydration *number* and *distance* as a chelate oscillates between hydrated and dehydrated forms over a period of observation. If dissociative exchange is slow then the chelate spends the majority of the period of observation with a water molecule closely associated with the chelate (q is high and r is short). However, if dissociative exchange is accelerated then this causes the chelate to cycle through the dehydrated form many more times over the course of the period of observation – decreasing q and increasing r . This change in q is inseparable from the associated change in r ; they occur simultaneously. For chelates that exchange extremely rapidly, such as *S*-SSSS-LnNB-DOTMA, it is more practical to discuss hydration of the chelate in terms of both number and distance of water, *i.e.* in terms of the hydration *state* (q/r^6) of the chelate

One important consideration not considered in Fig 5 is the relative energies of each chelate, intermediate and transition state of the exchange process. The relative energies of each structure will have a determining impact both on the rate of dissociative exchange and the lifetime of the dehydrated chelate. However, in the context of this work, in which the exchange behaviour of a chelate is compared only with itself, we are able to omit this consideration. Thinking about dissociative exchange in this way (Fig 5) provides a rational explanation for the changes in hyperfine shift of the EuNB-DOTMA chelates (Fig 2 and supplementary information Figs S3-7). As the temperature increases the rate of dissociative water exchange increases. As the rate of dissociative exchange increases the weighting of time-averaged conformation of all six chelates studied herein shifts such that they increasingly resemble the dehydrated form of the chelate. In other words as the rate of dissociative exchange increases the hydration state (q/r^6) of the chelate decreases. Of course, one could write that the hydration *number* is reduced. Alternatively, one could write that the value of r_{EuO} has increased. Mathematically, these expressions would amount to the same thing in terms of SBM theory; however, neither statement holds up to scientific scrutiny. This was the key conclusion of Parker's seminal paper on hydration – that hydration can only be described in terms of the number *and* position of water molecules.³³ Because it is impossible to quantify or distinguish the extent to which either of these parameters changes with variations in dissociative exchange rate the use of a single hydration parameter (q/r^6), as understood by Bertini⁴⁵ and Koenig,⁴⁶ is to be preferred. It is evident that as dissociative exchange becomes very fast exchange the hydration state of a chelate will decrease to a measurable extent and substantially impact relaxivity.²⁵ These decreases in hydration are

visible in the time-averaged conformation of the ligand by ^1H NMR, but *only* when obfuscating isomeric exchange motions, such as arm rotation or ring flip, are ‘frozen-out’ as is the case in LnNB-DOTMA chelates. As exchange accelerates the structure of these chelates “closes in” more closely resembling a dehydrated chelate. In other words the time-averaged structure of a rapidly exchanging chelate more closely resembles the recently published structure of HoDOTMA ($q/r^6 = 2823 \text{ nm}^{-6}$)⁴² than that of GdDOTMA ($q/r^6 = 4096 \text{ nm}^{-6}$).³¹ A similar effect has been observed in a related system published recently by Platas-Iglesias and co-workers.²¹ Thus, the chemist studying chelates that undergo very rapid dissociative water exchange should understand that changes in the dissociative water exchange rate are intrinsically linked to the hydration *state* of the chelate, both through static structural effects described by Parker and co-workers³³ and through the dynamic effects described herein.

Conclusions

Chemists can readily reconcile the idea that longer bond distances (weaker bonds) **cause** dissociative exchange processes to occur more rapidly. Herein, we discover that the **effect** of faster dissociative exchange is to further increase the average distance (not the ‘bond’ distance) of the water molecule from metal ion. This explains why the difference in metal-water distance between slowly and rapidly exchanging chelates increases from 2.8% in the solid to 4.5% in solution.^{31, 32} In short there is an intrinsic intertwining of a chelate’s hydration state (q/r^6), a structural parameter and water exchange ($1/\tau_M$), a dynamic parameter, that is more complex than provided for by a traditional view of the dissociative exchange mechanism. Two important points should be clearly stated:

- because the lifetime of the $q = 0$ state is very short indeed this effect is only likely to become apparent when exchange becomes exceedingly fast, *i.e.* τ_M becomes very short.
- the relationship between q/r^6 and τ_M is certain to be different for different coordination systems. The relative movement of ligand, metal and water during exchange will be unique for each chelate system. Furthermore, the relative energies of the chelate, and transition state and intermediate of the exchange process will differ as will depend upon ligand structure and strain. Other coordination systems will therefore have more, or less, pronounced relationships between these parameters than the square antiprisms studied herein.

The traditional picture of dissociative exchange separates structure and dynamics; however, careful consideration shows that they are inextricably linked. In solution structure is a 4-dimensional concept and the dynamics of a system forms an integral part of its structure. In consequence descriptions of lanthanide hydration should follow the precepts of Bertini⁴⁵ and Parker³³ and use a single parameter (q/r^6) to describe both the number and position of water molecules on the metal ion.

Experimental Section

All compounds and materials were prepared using previously described methods.^{32, 36} ^1H NMR data were acquired on a Bruker Avance IIa spectrometer operating at 400.13 MHz

using a 5 mm broadband probe. All NMR samples were prepared in >99.9% enriched D₂O and the pD was not adjusted but found to lie in the region of 3 – 4 depending upon the concentration of the chelate (each chelate is isolated in its HEuL(H₂O) form by preparative HPLC). The temperature was controlled using the installed variable-temperature controller model 2416 with BCU-05 chiller. Acquisition parameters were adjusted as the temperature was increased to account for the change in magnetic properties with changing temperature: the acquisition time varied from 0.21-0.23 s; the relaxation delay varied from 0.5-1.4 s; and the number of scans varied from 64 to 256. All spectra were referenced with the HOD at 4.7 ppm. Spectral assignments were made on the basis of COSY NMR spectra recorded for each chelate at 278 and 313 K.³⁷

Supplementary Material

Refer to Web version on PubMed Central for supplementary material.

Acknowledgments

The authors thank the National Institutes of Health (EB-11687), Oregon Nanoscience and Microtechnologies Institute (N00014-11-1-0193), Portland State University and the Oregon Opportunity for Biomedical Research for financial support of this work.

references

1. Langford, CH.; Gray, HB. *Ligand Substitution Processes*. W.A. Benjamin; New York: 1966.
2. Powell DH, Ni Dhubhghaill OM, Pubanz D, Helm L, Lebedev YS, Schlaepfer W, Merbach AE. *J. Am. Chem. Soc.* 1996; 118:9333–9346.
3. Caravan P, Ellison JJ, McMurry TJ, Lauffer RB. *Chem. Rev.* 1999; 99:2293–2352. [PubMed: 11749483]
4. Baranyai Z, Botta M, Fekete M, Giovenzana GB, Negri R, Tei L, Platas-Iglesias C. *Chem. Eur. J.* 2012; 18:7680–7685. [PubMed: 22615142]
5. Werner EJ, Datta A, Jocher CJ, Raymond KN. *Angew. Chem., Int. Ed.* 2008; 47:8568–8580.
6. Aime S, Calabi L, Cavallotti C, Gianolio E, Giovenzana GB, Losi P, Maiocchi A, Palmisano G, Sisti M. *Inorg. Chem.* 2004; 43:7588–7590. [PubMed: 15554621]
7. Muller RN, Raduchel B, Laurent S, Platzek J, Pierart C, Mareski P, Vander Elst L. *Eur. J. Inorg. Chem.* 1999:1949–1955.
8. Dunand FA, Borel A, Merbach AE. *J. Am. Chem. Soc.* 2002; 124:710–716. [PubMed: 11804502]
9. Caravan P, Astashkin AV, Raitsimring AM. *Inorg. Chem.* 2003; 42:3972–3974. [PubMed: 12817950]
10. Bloembergen N. *J. Chem. Phys.* 1957; 27:572–573.
11. Bloembergen N, Morgan LO. *J. Chem. Phys.* 1961; 34:842–850.
12. Bloembergen N, Purcell EM, Pound RV. *Phys. Rev.* 1948; 73:679–712.
13. Solomon I. *Phys. Rev.* 1955; 99:559–565.
14. Solomon I, Bloembergen N. *J. Chem. Phys.* 1956; 25:261–266.
15. Laus S, Ruloff R, Toth E, Merbach AE. *Chem. Eur. J.* 2003; 9:3555–3566. [PubMed: 12898682]
16. Congreve A, Parker D, Gianolio E, Botta M. *Dalton Trans.* 2004:1441–1445. [PubMed: 15252639]
17. Rudovsky J, Cigler P, Kotek J, Hermann P, Vojtisek P, Lukes I, Peters JA, Vander Elst L, Muller RN. *Chem. Eur. J.* 2005; 11:2373–2384. [PubMed: 15685711]
18. Laurent S, Vander Elst L, Vroman A, Muller RN. *Helvetica Chimica Acta.* 2007; 90:562–573.
19. Lebduskova P, Hermann P, Helm L, Toth E, Kotek J, Binnemans K, Rudovsky J, Lukes I, Merbach AE. *Dalton Trans.* 2007:493–501. [PubMed: 17213936]

20. Polasek M, Sedinova M, Kotek J, Vander Elst L, Muller RN, Hermann P, Lukes I. *Inorg. Chem.* 2009; 48:455–465. [PubMed: 19090686]
21. Rodriguez-Rodriguez A, Esteban-Gomez D, de Blas A, Rodriguez-Blas T, Fekete M, Botta M, Tripier R, Platas-Iglesias C. *Inorg. Chem.* 2012; 51:2509–2521. [PubMed: 22243216]
22. Laus S, Sour A, Ruloff R, Toth E, Merbach AE. *Chem. Eur. J.* 2005; 11:3064–3076. [PubMed: 15776490]
23. Rudovsky J, Botta M, Hermann P, Hardcastle KI, Lukes I, Aime S. *Bioconjug. Chem.* 2006; 17:975–987. [PubMed: 16848405]
24. Tei L, Gugliotta G, Baranyai Z, Botta M. *Dalton Trans.* 2009:9712–9714. [PubMed: 19885512]
25. Avedano S, Botta M, Haigh J, Longo LD, Woods M. *Inorg. Chem.* 2013; 52:8436–8450. [PubMed: 23841587]
26. Aime S, Botta M, Ermondi G. *Inorg. Chem.* 1992; 31:4291–4299.
27. Hoefl S, Roth K. *Chem. Ber.* 1993; 126:869–873.
28. Woods M, Aime S, Botta M, Howard JAK, Moloney JM, Navet M, Parker D, Port M, Rousseaux O. *J. Am. Chem. Soc.* 2000; 122:9781–9792.
29. Aime S, Barge A, Bruce JI, Botta M, Howard JAK, Moloney JM, Parker D, de Sousa AS, Woods M. *J. Am. Chem. Soc.* 1999; 121:5762–5771.
30. Woods M, Kovacs Z, Zhang S, Sherry AD. *Angew. Chem. Int. Ed.* 2003; 42:5889–5892.
31. Aime S, Botta M, Garda Z, Kucera BE, Tirso G, Young VG, Woods M. *Inorg. Chem.* 2011; 50:7955–7965. [PubMed: 21819052]
32. Woods M, Botta M, Avedano S, Wang J, Sherry AD. *Dalton Trans.* 2005:3829–3837. [PubMed: 16311635]
33. Beeby A, Clarkson IM, Dickins RS, Faulkner S, Parker D, Royle L, de Sousa AS, Williams JAG, Woods M. *J. Chem. Soc., Perkin Trans 2.* 1999:493–504.
34. Di Bari L, Pescitelli G, Sherry AD, Woods M. *Inorg. Chem.* 2005; 44:8391–8398. [PubMed: 16270977]
35. Aime S, Botta M, Parker D, Williams JAG. *J. Chem. Soc., Dalton Trans.* 1996:17–23.
36. Tirso G, Webber BC, Kucera BE, Young VG, Woods M. *Inorg. Chem.* 2011; 50:7966–7979. [PubMed: 21819053]
37. Webber BC, Woods M. *Inorg. Chem.* 2012; 51:8576–8582. [PubMed: 22809081]
38. Piguet C, Geraldes CFGC. *Handbook on the Physics and Chemistry of Rare Earths.* 2003; 33:353–463.
39. Dickins RS, Parker D, Bruce JI, Tozer DJ. *Dalton Trans.* 2003:1264–1271.
40. Ren J, Zhang S, Sherry AD, Geraldes CFGC. *Inorg. Chim. Acta.* 2002; 339:273–282.
41. Kotek J, Rudovsky J, Hermann P, Lukes I. *Inorg. Chem.* 2006; 45:3097–3102. [PubMed: 16562966]
42. Payne KM, Aime S, Botta M, Valente E, Woods M. *Chem. Commun.* 2013:2320–2322.
43. Pollet R, Nair NN, Marx D. *Inorg. Chem.* 2011; 50:4791–4797. [PubMed: 21520891]
44. Parker D, Dickins RS, Puschmann H, Crossland C, Howard JAK. *Chem. Rev.* 2002; 102:1977–2010. [PubMed: 12059260]
45. Banci L, Bertini I, Luchinat C. *Inorg. Chim. Acta.* 1985; 100:173–181.
46. Koenig SH, Epstein M. *J. Chem. Phys.* 1975; 63:2279–2284.

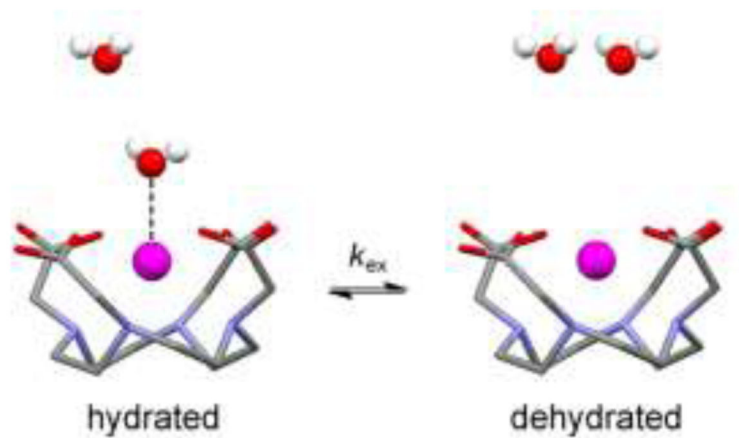


Fig 1. The “traditional” picture of the dissociative solvent exchange mechanism and of water exchange in monohydrated Gd^{3+} chelates in particular. The effect of exchange on the ‘structure’ of the chelate is generally neglected.

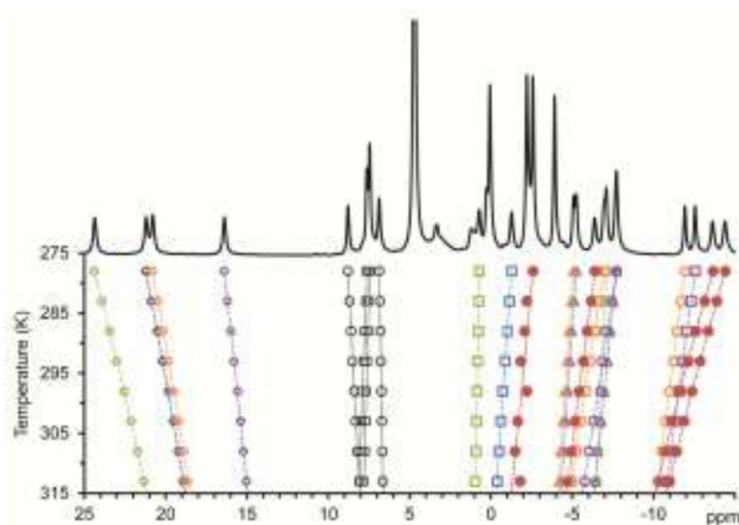


Fig. 2. Variable temperature ^1H NMR shifts of the ‘corner’ isomer *S*-SSSS-EuNB-DOTMA recorded in D_2O at 400 MHz. The spectral assignment from COSY data (reported elsewhere)³⁷ allows each proton of each ethylene bridge to be shown in the same color using open symbols according to the scheme: ax^S (diamonds); eq^S (squares); ax^C (triangles); eq^C (circles) (see also Fig 4 and supplementary information, S1). The acetate protons, ac, are shown as closed red circles; the benzylic protons as black open circles; and the aromatic protons as black open squares. For clarity the temperature dependence of the methyl substituents is not shown.

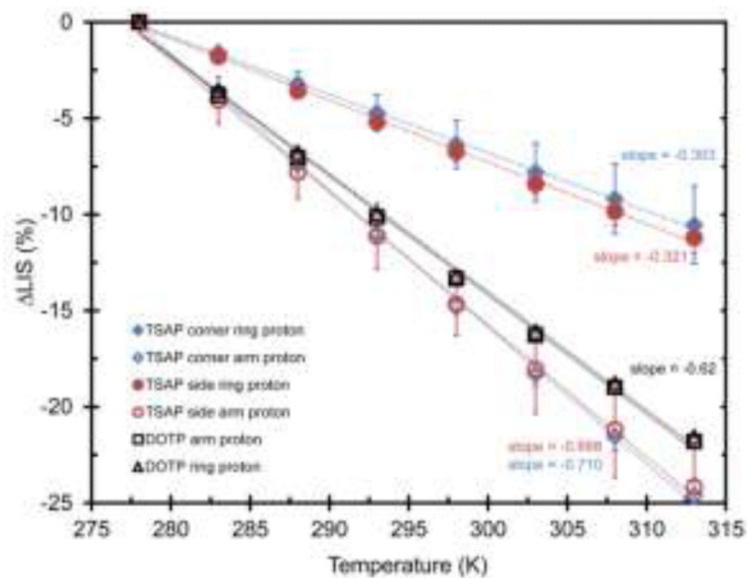


Fig. 3.

The change in experimentally observed lanthanide induced shift (LIS) with changing temperature for the ring proton (ax^S) and pendant arm proton (ac) of the ‘side’ and ‘corner’ isomers of EuS-SSSS-NB-DOTMA (SAP) expressed as a percentage of the shift at 278 K. The error bars represent the experimentally observed deviation from the average value for each data point. The data are shown against those obtained for EuDOTP for comparative purposes.

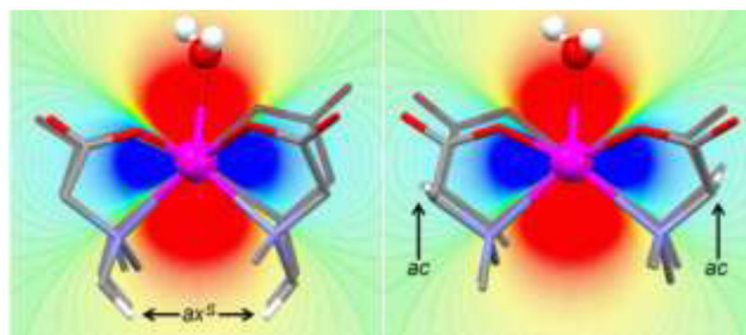


Fig. 4. Cross-sections of the mono hydrated (front) and dehydrated (shadow, back) structures of the TSAP isomer of YDO3AP(ABn) centered on a heat map of the axial dipolar contribution (proportional to $G = 3\cos^2\theta - 1/r^3$). Blue indicates an up-field shift and red a down-field shift. These depictions visually represent the change in the axial dipolar shift experienced by the ax^S (left) and ac (right) protons of the chelates.

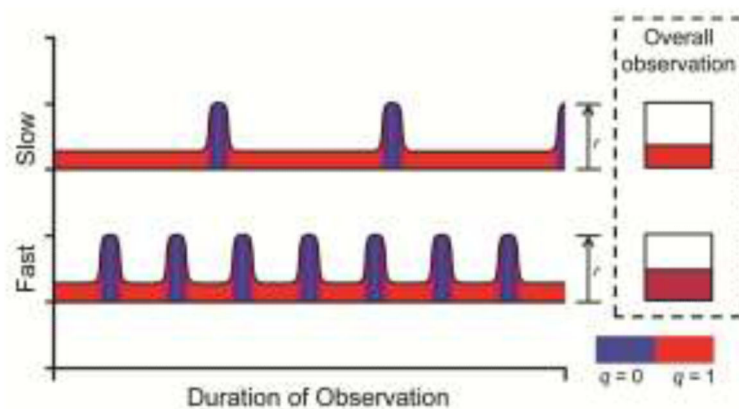


Fig. 5.

A representation of the time spent in the hydrated (red) and dehydrated (blue) forms over a period of observation for a rapidly and a slowly exchanging “ $q = 1$ ” Gd^{3+} chelate. On the right is shown the resultant time averaged observed values of hydration state (represented by the average colour over the observation window) and metal water distance r , (represented by the height of the coloured area). It is clear that more rapid exchange gives rise to a longer time-averaged value of r , and a slightly reduced time-averaged hydration state. It should be noted that the lifetime of the $q = 0$ state in this figure is exaggerated for illustrative purposes, it is not proposed that the $q = 0$ has a lifetime proportionately as long as shown in reality. Furthermore, the trajectory of the water molecule through exchange process is also unknown, a single representation is shown here to emphasize that the water molecule cannot jump from the metal to the bulk without passing through the intervening space.

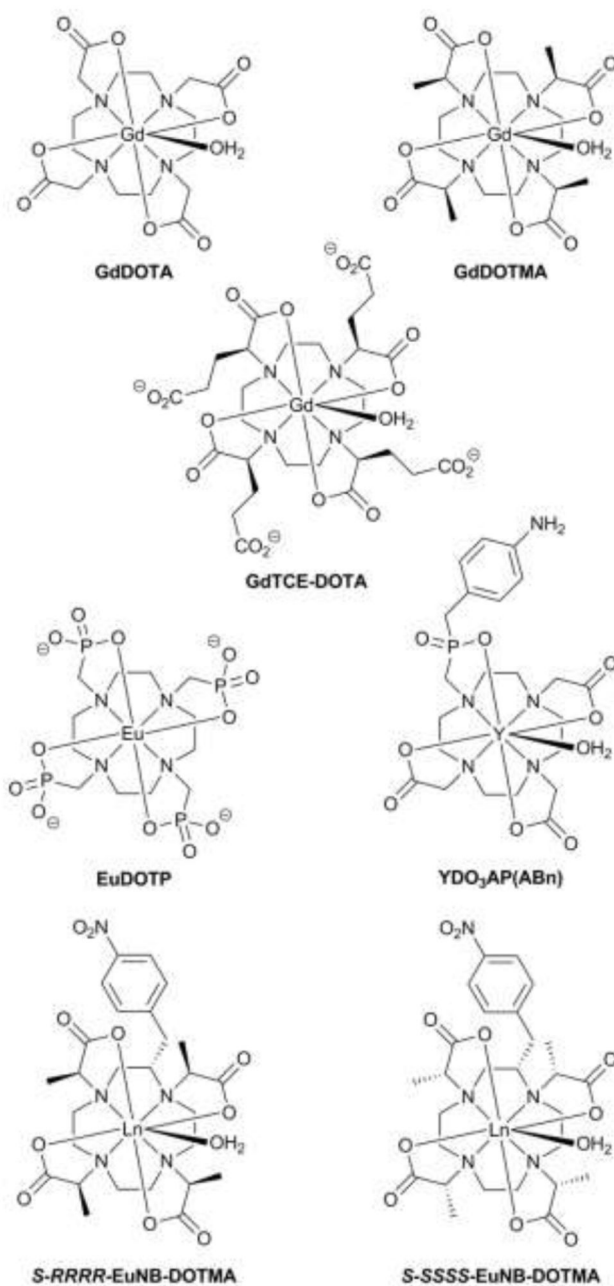
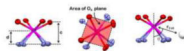


Chart 1.
The structures of chelates discussed herein

Table 1

Selected parameters from the crystal structures of dehydrated and mono hydrated YDO3AP(ABn).⁴¹ Since these chelates are asymmetric the values given for the positions of protons are average values, the naming system used for the protons is shown in Fig 4. G , the axial geometric parameter = $3\cos^2\theta - 1/r^3$.



	mono-hydrated	dehydrated
q	1	0
Y-OH ₂ (Å)	2.485	N/A
c (Å)	2.421	2.559
d (Å)	1.660	1.531
d/c	0.69	0.60
N ₄ -O ₄ (°)	26.79	-26.08
N-C-C-N (°)	56.67	-57.95
Area of O ₄ plane (Å ²)	9.55	8.31
ac		
r _{YH} (Å)	3.43	3.47
θ (Å)	81.68	82.85
G (×10 ³)	-22.88	-23.21
G _{q=1} - G _{q=0} (×10 ³)		-0.33
ax^s		
r _{YH} (Å)	3.66	3.68
θ (°)	14.55	25.07
G (×10 ³)	29.26	36.88
G _{q=1} - G _{q=0} (×10 ³)		7.62